Transactions of the **14th International Conference on Structural Mechanics in Reactor Technology** (SMiRT 14), Lyon, France, August 17-22, 1997

GW/1

Modelling of scatter and size effects in ductile and brittle fracture

Pineau A.
URA CNRS 866, France

ABSTRACT

It is well established that the strain to failure of smooth and notched bars or the fracture toughness of structural steels may be largely scattered. Moreover a size effect is usually observed : the ductility or the fracture toughness decrease with increasing size of the specimens. This scatter and size effects are one of the most serious problems encountered in the transferability of test results obtained on laboratory specimens to components. The present paper is an attempt to provide some guidelines to deal with this problem. The methodology adopted is that of the *local approach to fracture* based on the quantitative description of the micromechanisms of fracture. Both brittle (cleavage) fracture and ductile rupture are considered with a special emphasis on the latter mode of fracture.

I. INTRODUCTION

The mechanical integrity of structures is usually assessed on the basis of relatively well accepted rules. These rules are based on elastic and elastic-plastic fracture mechanics. It is assumed that they are able to assess the mechanical integrity even for complex situations, including large-scale yielding, mixed mode fracture and non-isothermal loading situations, although these approaches may be questionable in these circumstances. The main problem which is raised is the transferability of laboratory test results to components. The standards for laboratory tests of fracture toughness K_{IC} measurements are largely used in spite of the fact that the fracture toughness, even under plane strain small-scale yielding conditions, is a decreasing function of specimen thickness. This size effect is simply related to the probability of finding a weak zone along the crack front which is an increasing function of specimen thickness. It is therefore very doubtful that the fracture toughness can be measured by a single global parameter, such as K or J.

More recently another approach to the problem has been developed. This is the so-called local approach in which the modelling of fracture toughness is based on local fracture criteria. These criteria are established from tests and microstructural observations carried out on notch round tensile specimens (see e.g.[1], [2]).

In this paper a brief overview of the micromechanisms of fracture is presented with the emphasis laid upon the sources of the observed scatter and size effects. Two fracture modes are considered successively : brittle fracture and ductile rupture. The paper is divided into two main parts. In the first part devoted to brittle fracture an attempt is made to show the main lines along which the fracture toughness in the lower shelf of the brittle-ductile transition curve can be modelled. This part is essentially based on results obtained on A508 PWR steel. The second part of the presentation concentrates only on ductile fracture. Two types of materials which are also largely used in nuclear reactors are considered : (i) a plain carbon steel in which ductile rupture is initiated from MnS inclusions, and (ii) a duplex ($\gamma+\delta$) stainless steel (CF8M) in which ductile fracture of austenite phase (γ) is initiated from cleavage microcracks formed in the ferrite phase (δ) when the material is submitted to a thermal embrittlement treatment.

II. BRITTLE FRACTURE

II.1. Physical background for Weibull statistics

The micromechanisms of cleavage fracture in steels have been reviewed by several authors (see e.g. [1]). In a material for which there is no change in deformation modes with temperature, that is, in which cleavage is always slip induced, it can be assumed that within a first approximation, brittle fracture takes place when the maximum principal stress reaches a critical value, σ_C. Several models have been proposed to account for the value of σ_C ($\simeq$ 1500 MPa in structural steels). One important aspect related to cleavage fracture is the existence of a relatively large scatter in the test results. This situation, very well known in other brittle materials, like ceramics, does not seem to have been given enough attention in steels for a long time. For an homogeneous material in which there is no statistical spatial correlation between two adjacent areas, the Weibull weakest link hypothesis is well accepted to account for brittle fracture. This was the basis of the model proposed by Beremin [3] and Wallin [4,5]. If it is assumed that the materials contain microdefects (cracked carbides, cracked or debonded inclusions, single grain microcracks etc...) of length a, such as their length has a given probability distribution P(a) da where P(a) is proportional to a^{-n}, it can easily be shown [6] that, according to the weakest link theory, the probability to fracture, P_R, of a specimen of volume V submitted to an homogeneous stress state, σ, is given by :

$$P_R = 1 - \exp - \left(\frac{\sigma^m \ V}{\sigma_u^m \ V_u} \right) \tag{1}$$

where V_u is an arbitrary unit volume, σ_u is the average cleavage strength of that unit volume, while m is the shape factor of the Weibull expression. It can also be shown that there exists a simple relation between m and n, since :

$$m = 2n - 2 \tag{2}$$

Eq. 1 is a simplified expression which contains no cut-off parameter. In 3 dimensions and in the presence of smooth stress gradients, this equation can be expressed as :

$$P_R = 1 - \exp \left[- \frac{\int_{PZ} \sigma_1^m \ dV}{\sigma_u^m \ V_u} \right] \tag{3}$$

where σ_1 is the maximum principal stress while the volume integral is extended over the plastic zone PZ. The latter expression can be rewritten as :

$$\sigma_W = \sqrt[m]{\int_{PZ} \sigma_1^m \frac{dV}{Vu}} = \sigma_u \sqrt[m]{\left(\mathrm{Log} \frac{1}{1 - P_R} \right)} \tag{4}$$

where σ_W is referred to as the "Weibull stress". It is worth noting that Eq.1 contains only two independent parameters, m and the product $\sigma_u^m V_u$. The values of m and σ_u are usually determined from tests on notched bars. In a tempered bainitic C-Mn-Ni-Mo steel (A508) it was found that m = 22, while σ_u was dependent on the microstructure of the material [3]. It should also be noticed that the volume V_u is related to some extent to the characteristic distance (a few grain sizes) used in the Ritchie, Knott and Rice model [7].

More recently a similar statistical approach has been applied to account for brittle intergranular fracture in A508 steel resulting from temper embrittlement [8,9]. In these studies it was shown that the parameter σ_u was a slightly increasing function of temperature. This apparent temperature dependence was tentatively explained as arising from the inhomogeneity in plastic deformation of polycrystals. Still more recently in another study, it was shown that the scatter in test results and the size effect could be explained by the existence of two types of weak links : grain boundaries and large MnS inclusions [10]. In both cases a Weibull type statistical model was used to describe the probability of finding these defects. The integration of expressions similar to Eq.3 was extended over the plastic zone for the defects related to the distribution of weak grain boundaries while that corresponding to inclusions was made not only over this plastic zone but also over the areas which were elastically deformed since the inclusions are poorly bounded to the matrix. This reproduced the temperature dependence observed for the fracture toughness.

II.2. Modelling fracture toughness

The application of this model to the crack-tip situation is straightforward if it assumed that the stress-strain field ahead of the crack tip under small scale yielding conditions is simply scaled by the ratio $x/(K/\sigma_Y)^2$ or $x/(J/\sigma_Y)$, where x is the distance ahead of the crack-tip and σ_Y the yield strength of the material [1,3,11]. The probability distribution for the fracture toughness can then be expressed as :

$$P_R = 1-\exp -\left[\frac{K_{IC}^4\, B\, \sigma_Y^{m-4}\, C_m}{V_u\, s_u^m}\right] \tag{5}$$

where B is the specimen thickness and Cm is a numerical factor. As shown earlier [3,12,13] the predicted variations of K_{IC} with specimen thickness, temperature and strain rate - via the temperature dependence of the yield strength - are in good agreement with the experimental results. Similarly the statistical effects of thickness can be taken into account by applying a model proposed by Wallin [14], based on a three parameter Weibull distribution of the cleavage fracture toughness. This author has proposed a model which takes into account the specimen thickness and a certain ductile crack growth preceding brittle cleavage fracture. In the case of no ductile growth the fracture probability P_R can be expressed as :

$$P_R = 1-\exp -\left[\frac{B}{B_o}\left(\frac{K_{IC} - K_{Min}}{K_o - K_{Min}}\right)^4\right] \tag{6}$$

where B_o is an arbitrary (normalization) thickness, K_o is a distribution parameter depending on B_o as well as on temperature, and K_{Min} is a limiting value below which fracture is impossible.

To conclude this part devoted to brittle fracture it can be added that the above approach has been applied to three-dimensional cracks [6] and to non-isothermal tests, including thermal shock experiments [15] as well as experiments involving a warm-prestresss effect [16]. More recently this approach was also successfully applied to interpret the shift of the brittle-ductile transition related to the short crack effect observed in fracture toughness tests [17]. In all these cases a closed form as simple as Eq.5 could not be derived since these complex loading modes required numerical calculations, as shown elsewhere [18].

III. DUCTILE FRACTURE

III.1. Introduction to ductile rupture

When modelling ductile rupture numerous material parameters have to be determined for the comparison of the results of simulations and experiments. In the present study an attempt is made to show that relevant microstructural dáta can be used to reduce the number of "fitting parameters". Modelling of ductile rupture can be done using two widely different approaches [19]. The first approach consists in carrying out simulations of the mechanical response of structures assuming that the constitutive equation of the material is not affected by damage. This is therefore an "*uncoupled*" approach in which a local rupture criterion is applied to the structure in a post-processor routine. The second approach ("*coupled*") is based on continuum damage mechanics using models for damaging materials such as those proposed by Tvergaard and Rousselier [20,21]. In this case the effect of damage evolution on stress distribution can be fully accounted for. The "uncoupled" approach has been largely developed (see eg. [11,22]). In the following, the coupled approach is used since interactions between damaged zones, which lead to premature failure in highly inhomogeneous structures, can be taken into account [23].

III.2. Materials and experimental procedures

The results obtained on two widely different materials are reported. The first material is a plain carbon steel containing MnS inclusions which easily debond from the matrix. In this steel the process of ductile rupture is therefore essentially void growth controlled. Detailed results on this material are given elsewhere [24,25]. Here it is enough to say that the distribution of inclusion volume fraction f_o was represented by a Γ-distribution :

$$G(f_o) = \frac{1}{\beta^\alpha\ \Gamma(\alpha)}\ f_o^{\alpha-1}\ \exp\left(\frac{f_o}{\beta}\right),\ \text{with}\ \alpha = 1.14\ \text{and}\ \beta = 0.22\,10^{-2} \qquad (7)$$

MnS inlusions were observed to be grouped in clusters, the average distance between clusters being equal to 250 μm. Specimens for mechanical tests were taken from two different parts of a large component (GU2 and GV2, respectively) having the same inclusion content but slightly different stress-strain curves.

The second material is a cast ferrite (δ)-austenite (γ) duplex stainless steel. In this steel cleavage microcracks are continuously nucleated in the embrittled ferrite so that final fracture is essentially void nucleation controlled. Detailed results are reported elesewhere [2,11,25,26]. The microstructure of this alloy can be described as a mixture of two interconnected phases δ and γ, with a volume fraction of the ferrite phase of about 30%. The hardness of the δ phase after long thermal aging treatment at 350/400°C is much larger than that of the ductile γ phase. Interrupted tensile tests showed that cleavage of the ferrite phase was essentially controlled by plastic strain [11]. Assuming that a cleavage microcrack initiated in the δ phase is equivalent to a spherical cavity with the same projected area [27], the effective porosity due to nucleation (f_n) is related to plastic strain, p, by :

$$f_n = A_n\, p \qquad (8)$$

with A_n being uniformly distributed between 0.1 and 1.0.

Both materials were tested using smooth and notched axisymmetric bars referenced as AEχ with χ being equal to 10 x rd/ϕ_o where rd is the notch radius and ϕ_o the minimum diameter. These specimens allow the development of different stress triaxiality ratios in the center of the minimum section. Size effect was studied using homothetic notched bars with the same χ ratio. Charpy specimens (U, V notched and precracked) were also used to test the duplex stainless steel. Tests were performed at 20°C on the stainless steel and at 320°C on the carbon steel. The ductility of tensile bars is characterized by the mean strain to failure, $\bar{\varepsilon}_R = 2\log(R_o/R)$ where Ro is the initial redius of the minimum section and R its value at the onset of failure. On Charpy specimens the fracture toughness was divided into the energy necessary to initiate a macro-crack from the notch and the energy dissipated during crack growth. The size effect observed with these specimens was studied by varying the specimen thickness, B, keeping the in-plane dimensions, with B = 5 mm, 10 mm (conventional) and 20 mm.

III.3. Material modelling

Materials are modelled using continuum damage mechanics. Models are based on plastic criteria depending on porosity introduced by Gurson and Rousselier. The Gurson-Tvergaard criterion [20] is given by :

$$\Phi = \frac{\sigma_{eq}^2}{\sigma_*^2} + 2q_1 f^* \cosh\left(\frac{3q_2\sigma_m}{2\sigma_*}\right) - 1 - q_1^2 f^{*2} \tag{9}$$

The Rousselier criterion [21] is given by :

$$\Phi = \frac{\sigma_{eq}}{(1-f)\sigma^*} + \frac{\sigma_1}{\sigma^*} f\, D \exp\left(\frac{\sigma_m}{(1-f)\sigma_1}\right) - 1 \tag{10}$$

σ_{eq} is the Von Mises equivalent stress, σ_m the mean stress, f the porosity. σ^* is the yield stress of the undamaged matrix computed assuming isotropic hardening. q_1, q_2, D and σ_1 are material constants. The function f* was introduced [20] to account for the coalescence of adjacent voids which starts after a critical void volume fraction f_c is reached.

$$f^* = \begin{cases} f & \text{if } f < f_c \\ f_c + \delta(f - f_c) & \text{if } f > f_c \end{cases} \qquad \text{(carbon steel)} \tag{11}$$

In Eq. 11 δ is an "accelerating factor" introduced to "simulate" the final stage of ductile failure. This is a modification of the "original" Gurson model [28] for which f* = f. The evolution of porosity is given by the mass conservation :

$$\dot{f} = (1-f)\ \text{trace}\left(\dot{\bar{\varepsilon}}_p\right) \tag{12}$$

where $\dot{\bar{\varepsilon}}_p$ is the plastic strain rate tensor obtained assuming that plastic flow is normal to the yield surface. In the case of the duplex steel, the function f* is written as :

$$f^* = f + f_n \qquad \text{(duplex steel)} \tag{13}$$

where f_n is given by Eq.8. As damage nucleation rate is high, coalescence does not play an important role in the fracture process of this material. Note that, in this case, the evolution of f_n is solely determined from microstructural examinations so that no parameter fitting is needed. In particular no accelerating factor is needed.

The carbon steel was modelled using both Gurson-Tvergaard and Rousselier potentials with the following parameters : $f_c = 0.4\%$, $\delta = 3$, $\sigma_1 = 240$ MPa and $D = 1.5$. These parameters were adjusted to reproduce the experimental mean ductility on the smallest notched bar (ϕ_o = 3.75 mm). The duplex steel was modelled using the "original" Gurson potential and Eq.13. In both cases, $q_1 = 1.5$ and $q_2 = 1$ which are values commonly used in the literature.

To account for random distributions of inclusions (Carbon steel) or cleavage microcracks (Duplex steel), the materials were represented as a 2D square grid. Each square is assigned an initial value (f_o or A_n) according to the statistical distribution determined experimentally. A Finite Element (FE) mesh is then superposed to this grid (Fig.1). Each Gauss point corresponds to a grid cell and a given value. The grid size is equal to 250 µm (average cluster distance) in the case of the carbon steel and to 1 mm (mean austenite grain size) for the duplex steel. Heterogeneities are therefore modelled using a characteristic length (grid size) and a statistical distribution.

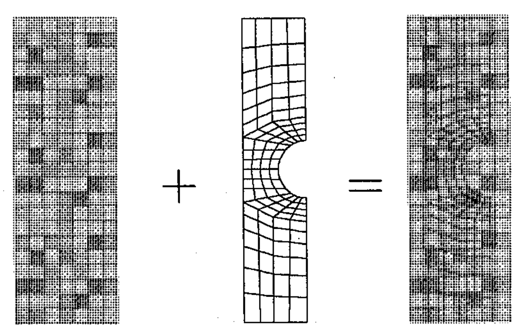

Figure 1 : Schematic representation showing how a random value is attributed to each Gauss point of a mesh.

All computations were performed using the Finite Element software ZeBuLoN7 developed in C++ at the Centre des Matériaux. 2D axisymmetric and plane strain simulations were carried out on notched bars and Charpy specimens respectively. Indeed the different zones are then modelled as ring or bars. 3D calculations should be used to avoid this effect. Preliminary 3D simulations indicate that 2D results can, in most cases, accurately represent the experimental data. Updated Lagrangian eight node quadratic elements with 4 Gauss points were used using a constant element size (500 µm) in regions where damage can develop.

III.4. __Results and discussion__

Effect of heterogeneities on ductility. Simulations of smooth tensile bars were carried out to investigate the effect of heterogeneities on ductile failure. Using data relative to the duplex steel, computations assuming a *uniform* crack nucleation rate were compared with computations done with the experimentally observed distribution. Fig.2 shows load-displacement curves computed for homogeneous nucleation rates $A_n = 0.1$ (minimum value), $A_n = 0.6$ (average value) and $A_n = 1.0$ (maximum value). It is shown that the simulation done with An = 0.1 overestimates both load and ductility; using An = 0.6 still overestimates ductility but allows to correctly describe the behaviour of the structure; on the other hand using An = 1.0 leads to an underestimation of the load and to a good evaluation of the average ductility. These computations clearly show that the inhomogeneity in the distribution of nucleation sites for ductile rupture must be taken into account. In the following solely the results obtained with *random distributions* (Fig.1) are reported. In Fig.2 the results obtained from 6 separate random drawings obtained with a Monte-Carlo type simulation are in good agreement with the experiments performed on smooth tensile bars.

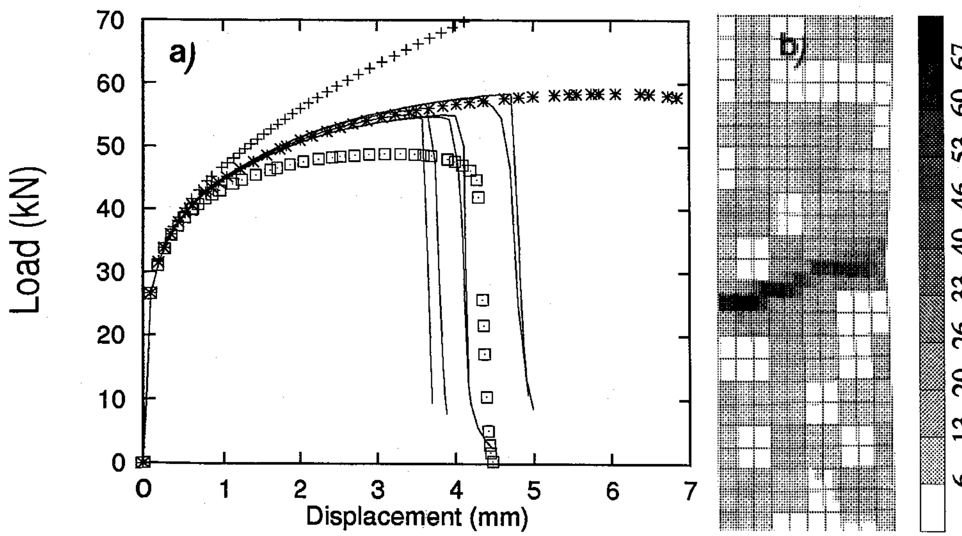

Figure 2 : Duplex Stainless Steel (a) Simulated Load-Displacement curves for the following conditions : (+) homogeneous nucleation with An = 0.1, (*) homogeneous nucleation with An = 0.6, ⊡ homogeneous nucleation with An = 1.0, (—) 6 separate random drawings for heterogeneous nucleation. (b) Damage (f* (%)) at Gauss points in the necking zone before rupture for an heterogeneous distribution of crack nucleation rate.

Round tensile bars : geometry effect. Smooth (AE∞), AE10, AE4 and AE2 specimens were tested. In all cases (ϕ_0) = 10 mm. Results are expressed as the mean strain to failure $\bar{\varepsilon}_R$. In the case of smooth bars, $\bar{\varepsilon}_R$ was measured in the necking zone. Fig.3 shows experimental ductilities together with simulated results for both steels. Stress triaxialities in the center of the notch are those computed assuming that materials are not damaged. In this figure it is observed that the experimental results are in good agreement with the numerical simulations. It can also be shown that the carbon steel obeys the McClintock [29], Rice and Tracey [30] criterion which assumes that the strain to failure is proportional to exp $(-3\tau/2)$ where $\tau = \sigma_m/\sigma_{eq}$ is the stress trraxiality ratio. On the other hand, the duplex steel whose failure is essentially governed by damage nucleation does not follow the above law.

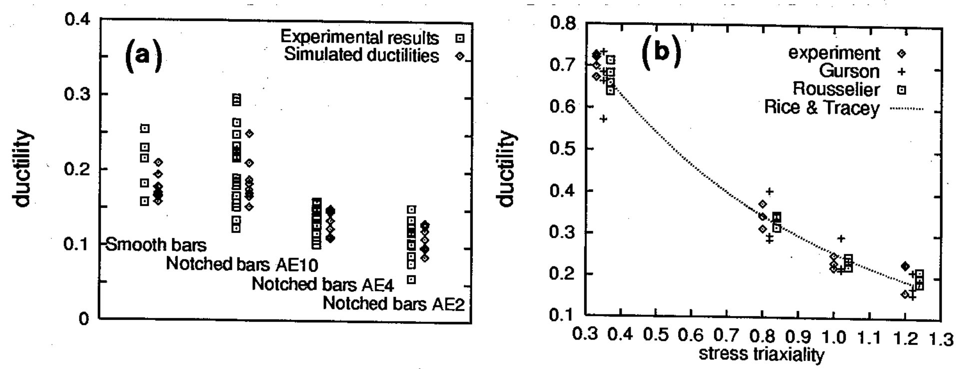

Figure 3 : Geometry effect on ductility : (a) duplex steel, (b) carbon steel (GU2 material).

Round tensile bars : size effect. Fig.4 shows experimental ductilities obtained for homothetic AE10 specimens having initial minimum diameters (ϕ_o) varying between 3.75 and 15 mm. A size effect is evidenced for both materials. It is shown that the average ductility as well as the scatter band width decrease as the specimen size is increased. Numerical results are also compared with experiments showing good agreement for both average values and scatter. For the carbon steel, better results were obtained using the Rousselier model.
Fig.4b also shows results obtained for a uniform distribution of initial porosity . They clearly indicate that mesh size effect can be neglected. This is due to the fact that strain and stress gradients in the notch region are smooth enough to be correctly described by a relatively small number of elements. Note however that notched bars are representative of crack initiation. For these geometries, crack propagation takes place without large dimensional changes of the notch geometry. On the other hand, a mesh size effect is observed on cracked specimens such as Compact Tension samples or Charpy specimens. Fig.5 illustrates the evolution of damage during loading on a AE10 specimen (duplex steel).

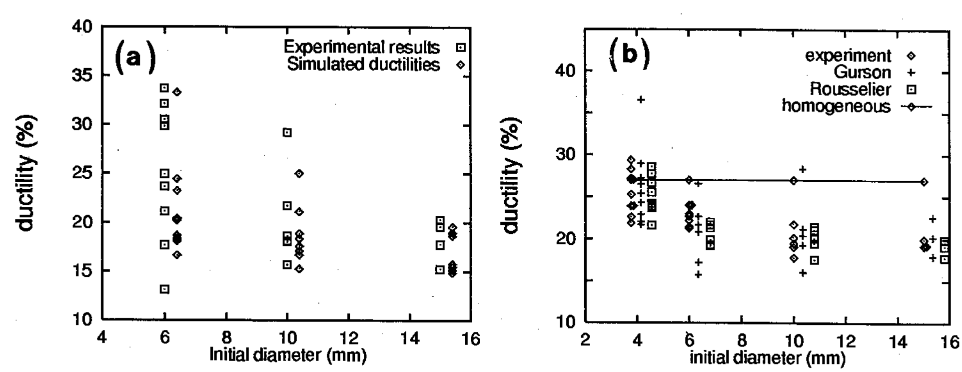

Figure 4 : Size effect on ductility : (a) duplex steel, (b) carbon steel (GV2 material).

Charpy specimens (Duplex stainless steel). Fig.6 shows experimental crack initiation energies measured on U and V-notched as well as precracked specimens, while the results of a numerical simulation of crack initiation and crack growth from a U notch is shown in Fig.7.

A large scatter is systematically observed. Size effects are also observed on U notched samples of different thicknesses. FE simulations, using a random distribution of damage nucleation rate, An, were made under plane strain conditions so that the size effect could not be represented. This would require 3D calculations. Our simulations, however, give a good approximation of experimental results. Further comparison between the simulations and the experiments were made for the crack propagation energy, E_p [25,26]. It was observed that E_p was almost constant, independent of specimen geometry ($E_p \simeq 16$ J/cm^2). The numerical simulations showed that those values of Ep could be reproduced adopting the average value of An (0.60). This was attributed to the fact that the crack propagates following an almost predefined path over the entire sample thickness.

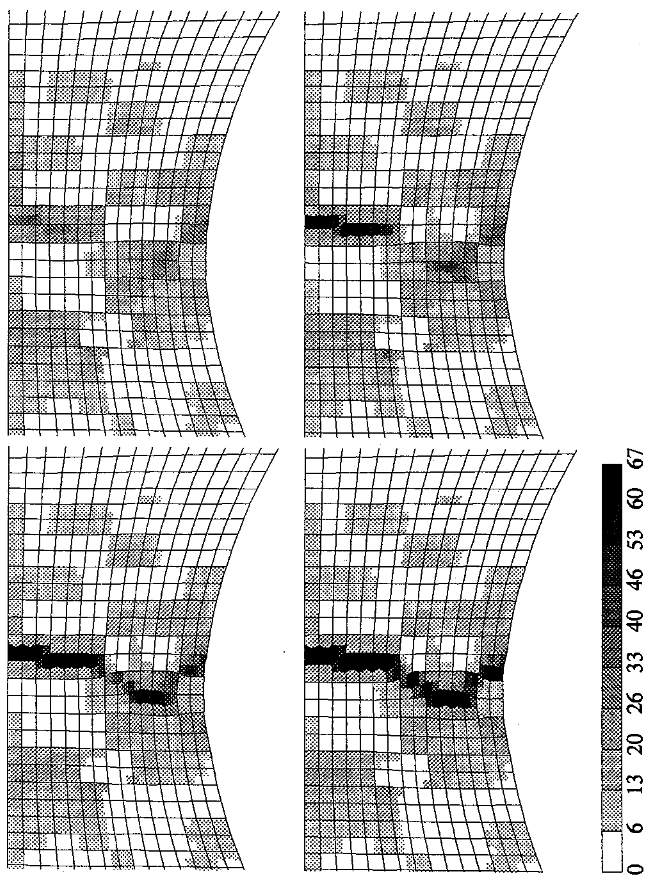

Figure 5 : Development of damage in a AE10 specimen during increasing loading (damage values (f* (%)) at Gauss points. Duplex stainless steel).

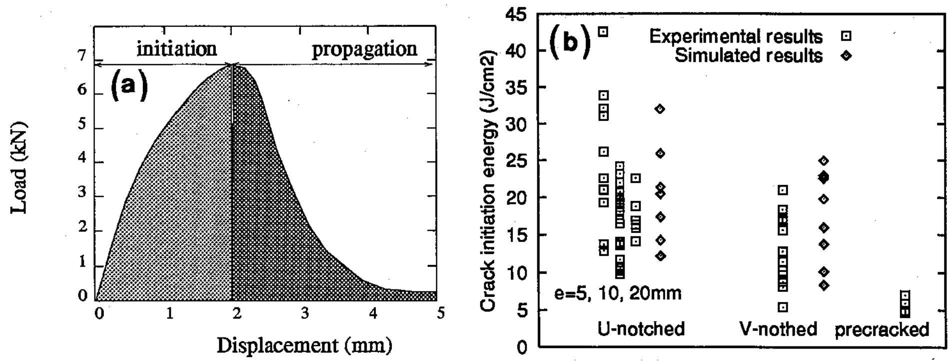

Figure 6 : (a) Definition of initiation and propagation energies, (b) results on U, V and precracked Charpy specimens and comparison with plane strain FE calculations.

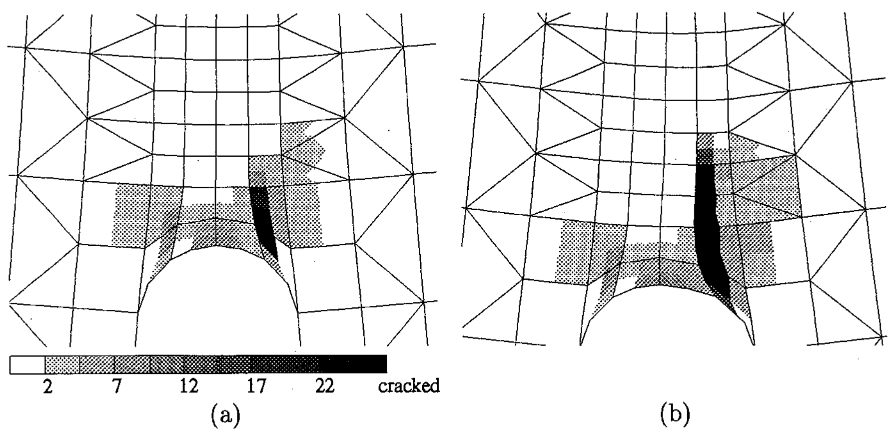

Figure 7 : Development of damage (f* (%)) in the notch region.

IV. CONCLUDING REMARKS

An attempt has been made to overview simple methods which take into account the role of material heterogeneites on brittle and ductile fracture. These methods require the distribution function of a number of material parameters (microdefects for cleavage and intergranular fracture, porosity and growth rate for ductile rupture) and a characteristic length. Both can be obtained from microstructual observations. These informations related to the materials are then used in a continuum damage model. Two types of models have been presented. In the first type no coupling effect between the constitutive equation and damage is taken into account. In the second type (Gurson and Rousselier potentials) damage is coupled to the constitutive equation.

These simple methods have been applied both to brittle and ductile fracture. In the first case the assumption of weakest link theory is the basis of the modelling. The simulation of ductile rupture of two widely different steels has been presented : (i) a plain carbon steel in which fracture is controlled by the growth of cavities nucleated from MnS inclusions, (ii) a duplex stainless steel in which cleavage crack initiation within the ferrite phase is the main damage mechanism.

The following results were obtained :
1. The method can be used to model both average ductilities (ductile rupture) or average fracture toughness (brittle fracture) and scatter observed on different specimen geometries. The method can also be used to represent the observed size effect.
2. Analysis of numerical resuls shows that material heterogeneities lower the strain to failure or the fracture toughness. This reduction in ductility is mainly due to the interaction between damaging zones. This clearly shows that homogeneization techniques cannot abruptly be used to model the fracture behaviour of multi-phase materials.
3. Use of relevant material data can largely reduce the number of parameters which have to be adjusted to model fracture. It is of primary importance for ductile rupture which requires numerous FE simulations of cracked specimens.

ACKNOWLEDGMENTS

The author would like to acknowledge Dr. J. Besson and all the PhD students of his research group, including in particular, L. Bauvineau, K. Decamp and L. Devillers-Guerville. Financial support from Electricité de France (EDF) is also greatfullly acknowledged. Thanks in particular to M. Bethmont, J.M. Freund, S. Jayet Gendrot and G. Rousselier from EDF.

REFERENCES

1. Pineau, A. 1981. Proc. 5th Int.Conf. on Fracture, Cannes (Edited by D. François et al), Pergamon Press, 2 : 533-577.

2. Pineau, A., P. Joly 1991. Defect Assessment in Components-Fundamentals and Applications, ESIS/EGF9 (Edited by J.G. Blauel and K.H. Schwalbe). MEP London : 381-414.

3. Beremin, F.M. 1983. A local criterion for cleavage fracture of a nuclear pressure vessel steel. Met. Trans., 14A : 2277-2286.

4. Wallin, K., T. Saario. & K. Törrönen 1984. Statistical model for carbide induced brittle fracture in steel. Metal Science, 18 : 13-16.

5. Wallin, K. 1991. Defect assessment in components-Fundamentals and Applications. ESIS/EFG9 (Edited by J.G. Blauel and K.H. Schwalbe), MEP, London : 415-445.

6. Mudry, F. 1987. A local approach to cleavage fracture. Nuclear Engineering and Design, 105 : 65-76.

7. Ritchie, R., J.F. Knott & J.R. Rice 1973. On the relationship between critical tensile stress and fracture toughness in mild steel. J. Mech. Phys. Solids, 21 : 395.

8. Kantidis, E., B. Marini, L. Allais & A. Pineau 1994. Validation of a statistical criterion for intergranular brittle fracture of a low alloy steel through uniaxial and biaxial (tension-torsion) tests. Int. J. of Fracture, 66 : 273-294.

9. Kantidis, E., B. Marini & A. Pineau 1994. A criterion for intergranular brittle fracture of a low alloy steel. Fatigue Fract. Engng. Mater. Struct. 17 : 619-633.

10. Yayhia, O., R. Piques & A. Pineau 1997. To be submitted.

11. Pineau, A. 1992. Topics in fracture and fatigue Ed. A.S. Argon Springer-Verlag : 197-234.

12. Wallin, K. 1984. The scatter in K_{IC} results. Engng Fract. Mech., 19 : 1085-1093.

13. Wallin, K. 1985. The size effect in K_{IC} results. Engng Fract. Mech., 22 : 149-163.

14. Wallin, K. 1989. The effect of ductile tearing on cleavage fracture probability in fracture toughness testing. Engng Fract. Mech. 32 : 523-531.

15. Di Fant, M., A. Genty & A. Pineau 1990. Thermal-schock-induced crack arrest of two low alloy steels. High Temperature Technology 8 : 105-114.

16. Beremin, F.M. 1981. Proc. 5th. Int. Conf. on Fracture, Cannes (Edited by D. François et al). Pergamon Press 2 : 825-832.

17. Tigges, D., R. Piques, J.M. Frund & A. Pineau 1994. Proc. ECF10 : Structural integrity : Experiments, models and applications (Edited by K.H. Schwalbe & C. Berger), Berlin : 637-646.

18. Mudry, F., F. Di Rienzo & A. Pineau 1989. Non linear Fracture Mechanics, vol.II. ASTM STP 995 (Edited by J.D. Landes et al) : 24-39.

19. Pineau, A. 1995. Mechanical Behaviour of Materials ICM7. Delf Univ. Press Delft. : 1-22.

20. Tvergaard, V. 1990. Material failure by void growth to coalescence. Advances in Applied Mechanics, 27 : 83-151.

21. Rousselier, G. 1987. Ductile fracture models and their potential in local approach to fracture. Nuclear Engineering and Design, 105 : 97-111.

22. Beremin, F.M., 1981. Cavity formation from inclusions in ductile fracture of A508 steel. Met. Trans., 12A : 723-731.

23. Becker, R. 1987. Effect of porosity distribution on ductile failure. J. Mech. Phys. Solids. 35 : 577-599.

24. Decamp, K., L. Bauvineau, J. Besson & A. Pineau 1997. To appear in Int. Journal of Fracture.

25. Besson, J. & A. Pineau 1997. Symp. "Recent Advances in Fracture" TMS Meeting Orlando, Fl, 9-13 Feb. 1997.

26. Devillers-Guerville, L., J. Besson & A. Pineau 1997. To appear in Nuclear Engineering and Design.

27. Gologanu, M., J.B. Leblond & J. Devaux 1994. J. Eng. Mat. Technol. : 116.

28. Gurson, A.L. 1977. J. of Engineering Materials and Technology, 99 : 2-15.

29. McClintock, F.A. 1971. Plasticity aspects of fracture, in Liebowitz H. editor, Fracture 3 : 47-225.

30. Rice, J.R. & D.M. Tracey 1969. J. Mech. Phys. Solids, 17 : 201-217.